Int. J. Electrochem. Sci., 15 **(2020)** 8450 – 8458, doi: 10.20964/2020.09.66

International Journal of
ELECTROCHEMICAL
SCIENCE
www.electrochemsci.org

Short Communication

Effect of Electroless Pretreatment on the Distribution of Etched Tunnels on Aluminum Foil

Haobin Wei [1], *Huining Huang* [1], *Ning Peng* [1,2,*], *Hehua Yao* [1]

[1] Guangxi Key Laboratory of Electrochemical and Magnetochemical Functional Materials, Guilin University of Technology, Guilin, 541004, China
[2] Institute of Technology Research and Development of Electronic Aluminum Foil, Guangxi Hezhou Guidong Electronics Technology Co. Ltd., 542800 Guangxi, China
[*]E-mail: ncdxclpn@glut.edu.cn

Received: 3 May 2020 / *Accepted:* 30 June 2020 / *Published:* 10 August 2020

The merged tunnels intensely reduced the specific surface area of etched aluminum foil using in aluminum electrolyte capacitor, which restrict the increase of the specific capacitance. In this paper, the nano-scale Sn nuclei was fabricated on aluminum surface by electroless plating to improve the surface area. The uniformly distributed Sn nuclei on aluminum surface could serve as the pitting initiation sites, due to the composition of Al-Sn localized micro-batteries. The distribution of the etched tunnels for the aluminum foil with proper Sn nuclei are improved significantly in contrast with that for the conventional aluminum foil, resulting in the enhancement of the specific surface area.

Keywords: Aluminum; SEM; Polarization; Pitting Corrosion;

1. INTRODUCTION

Direct current (DC) tunnel pitting of (100)-oriented aluminum foil in aggressive electrolytes has recently employed for enlargement of the specific surface area of aluminum foil used in high-voltage electrolytic capacitors [1, 2]. A high density of crystallographic etched tunnels (about 10^7 cm^{-2}), which mainly decide the specific surface area of the etched aluminum foil, can be generated on aluminum surface by using the DC tunnel etching [3, 4]. Because the capacitance of high-voltage electrolytic capacitors is primarily decided by the specific surface area of etched aluminum foil, the optimum of the specific surface area for etched aluminum foil must be achieved by controlling the distribution and sizes of the etched tunnels [5-8]. The effects of impurities such as Fe, Cu, Pb, Zn, etc, on etching behavior of aluminum foil has been well investigated [9-13]. And the uniformity of the etched tunnels has been enhanced by adjusting the impurity elements of the aluminum foil substrate [14, 15]. However, due to

the random and excess generation of the pitting initiation sites on the conventional aluminum surface, the uneven distribution of the etched tunnels and the merged tunnels (the cluster of the etched tunnels) formed on aluminum surface is hardly inevitable, which restrict the further enhancement of the specific surface area.

Recently, for the purpose of obtaining the optimal enlargement of the specific surface area, the tunnel etching of aluminum foil is still actively investigated to control the pitting initiation sites more precisely [5, 6, 16-18]. A patterned masking film and magnetron sputtering Cu were successfully fabricated on aluminum surface to control the pitting initiation sites accurately [16, 19]. An innovative method about high resolution inkjet printing was used to the site-controlled initiation of the etched tunnels on aluminum foil [17, 20]. These advanced technologies, which are relatively high-cost and low efficiency, can remarkably increase the specific surface area of etched aluminum foil. The purpose of the present work is to provide a novel way to improve the uniformity of etched tunnels on aluminum surface by using electroless Sn nuclei. The method using here was based on that the suitable density and relatively uniform distribution of Sn nuclei on aluminum foil surface could induce the generation of etched tunnels.

2. EXPERIMENTAL

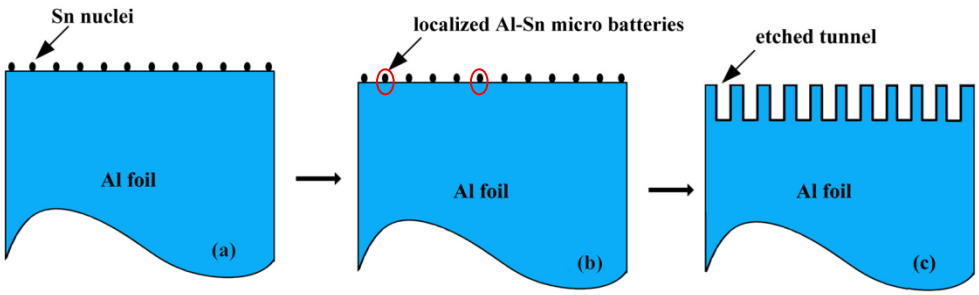

Figure 1. Schematic of formation of etched tunnels on aluminum foil using electroless Sn nuclei: (a) fabrication of Sn nuclei on aluminum surface, (b) the formation of Al-Sn localized micro-batteries and (c) DC etching of aluminum foil in 1 M HCl+3 M H_2SO_4 solutions at 70 ^oC.

Fig.1 shows the schematic of the formation of etched tunnels on aluminum foil by using the electroless Sn nuclei. The aluminium foil (JOINWORLD,China) used in this work was 120 μm thickness and 99.99 wt.% pure. The foil was fully annealed so that the {100} cubicity texture fraction was above 95%. In order to remove the enriched impurities and obtain a smoothing surface, the specimens were firstly electropolished at a voltage of 20 V in solutions of 10 vol.% $HClO_4$ + 90 vol.% ethanol at an ice-water bath for 30 s [21]. Then the polished specimens were fabricated Sn nuclei by electroless plating, which were proceeded in solutions of 1.5 M $Na_2SnO_3 \cdot 3H_2O$ +0.1 M NaOH+0.05 M $KNaC_4H_4O_6$ at different temperature for 80 s (Fig. 1a). As shown in Fig. 1b, the Sn nuclei and aluminum substrate could constitute localized Al-Sn micro-batteries, aimed at inducing the formation of etched tunnels. Finally, the as-received foils were DC etching under a constant current density of 250 mA cm^{-2} in solutions of 1

M HCl + 3 M H_2SO_4 at 70 ^oC, resulting in the uniform formation of etched tunnels on aluminum surface, as shown in Fig. 1c.

The surface morphologies of the Sn nuclei and the etched tunnels were observed by scanning electron microscopy (ZEISS, SUPPRA55). To compare the etchability of the aluminum foil with Sn nuclei and the conventional aluminum foil. An electrochemical cell of three electrodes was used for the electrochemical testing (Princeton Applied Research Potentiostat) of the foils in 1 M HCl + 3 M H_2SO_4 solution at 70 ^oC. The testing area of the foils were 1 cm^2 using epoxy resin coating. The working electrode (WE), counter electrode (CE) and reference electrode (RE) were carried out by the foils, Pt foil and a Ag/AgCl/sat. KCl electrode, respectively [22]. A scanning rate of 10 mV s^{-1} was used for testing the potentiodynamic polarization curve. The initial potential transient was conducted at a constant current density of 250 mA cm^{-2}. More than three times of measurements were carried out at the same conditions to ensure reproducibility.

3. RESULTS AND DISCUSSION

3.1. Morphology of the electroless Sn nuclei

Fig.2 shows the SEM images of the Sn nuclei prepared on the electropolished aluminum surface by electroless plating under the different temperature. It was thought best that the size of the generated Sn nuclei was nano-scale to avoid excess surface etching of aluminum foil.

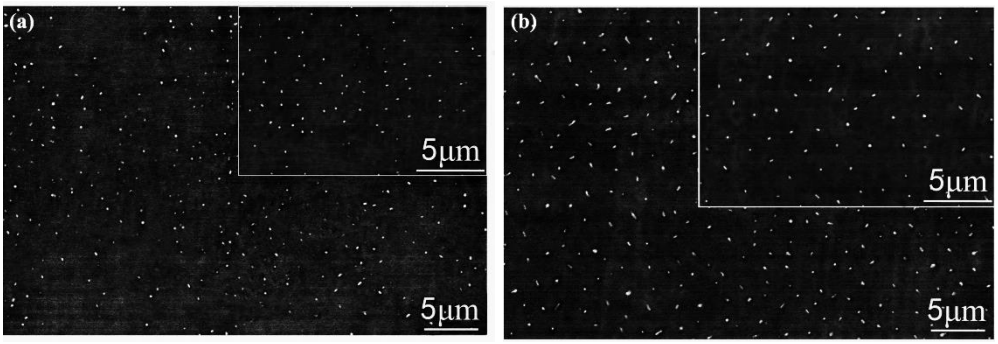

Figure 2. The SEM images of the Sn nuclei fabricated on the aluminum surface by electroless plating in solutions of 1.5 M $Na_2SnO_3 \cdot 3H_2O$ +0.1 M NaOH+0.05 M $KNaC_4H_4O_6$ at different temperature for 80 s: (a) 20 ^oC and (b) 30 ^oC.

As shown in Fig.2, the sizes of the Sn nuclei fabricated at the relatively low temperature were nano-scale. The nano-scale Sn nuclei in Fig.2a was infrequent and unevenly distributed on aluminum surface, due to the low surface activation at the low temperature. At the rising temperature, the density and uniformity of the Sn nuclei were enhanced clearly, as shown in Fig.2b. Besides, the size of the Sn nuclei at the high temperature was slightly larger than that at the low temperature, due to the increased nucleation and growth rate. It can be seen that by adjusting the solution temperature of electroless plating, the relatively proper density and uniform distribution of the Sn nuclei can be fabricated on the

electropolished aluminum surface. In the previous work, we found that the electrodeposited Zn nculei on the surface of aluminum foil can serve as the favorable sites for tunnel initiation on aluminum foil surface [23]. It can be seen that the size and distribution of the Sn nclei obtained from the electroless plating is more excellent than that of the Zn nuclei observed in the literature. Therefore, the aluminum foils with proper Sn nuclei will be generated the etched tunnel with more uniform distribution during the DC etching.

3.2. Surface morphologies of etched tunnels

Fig.3 shows the surface SEM images of the aluminum foil after the DC etching in solutions of 1 M HCl + 3 M H_2SO_4 at 70 ^oC for 20 s. The short etching time was to analyze the merged tunnels clearly. By comparing the etched morphology with Fig. 2, it indicates that the amount and distribution of etched tunnels on aluminum surface varies with the surface density of Sn nuclei.

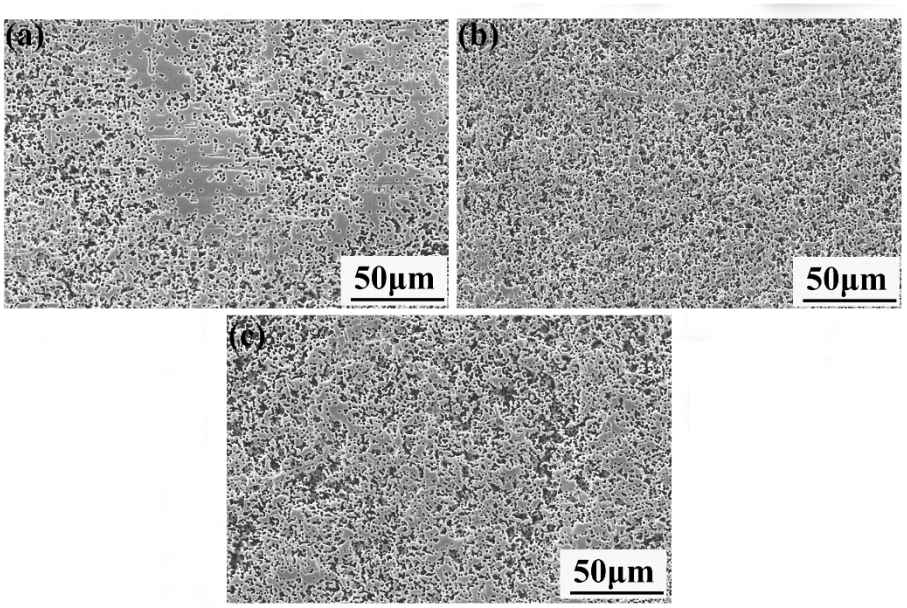

Figure 3. The SEM images of aluminum foil surface after DC etching: (a) the aluminum foil with low-density Sn nuclei, (b) the aluminum foil with proper Sn nuclei and (c) the conventional aluminum foil. DC etching was carried out in solutions of 1 M HCl+3 M H_2SO_4 at 70 ^oC for 20 s.

During the DC etching, the density and distribution of the Sn nuclei on the aluminum surface was found to strongly affects not only the density of the etched tunnels, but as well the distribution of the obtained tunnels. It can be seen from Fig.3a that the low-density Sn nuclei on aluminum surface resulted in the etched tunnels with low density and uneven distribution. However, when the aluminum foil with appropriate Sn nuclei was carried out DC etching, evenly distributed tunnels was observed on aluminum surface, as shown in Fig.3b. Moreover, few merged tunnels were generated on aluminum foil surface. The differences in density and distribution of Sn nuclei were relatively high between Fig.3a and Fig.3b, implying that they were the major factors responsible for the difference in etched morphology.

As for the conventional aluminum foil, due to the excess and random initiation of the etched tunnels, severely merged tunnels were generated on the conventional aluminum surface. It was implied from Fig. 3 that the Sn nuclei on aluminum surface can serve as the pitting initiation sites because of its role in anodically activating aluminum substrate in chloride etchant. So, the uniform distribution of the Sn nuclei on aluminum surface can facilitate the uniform distribution of the etched tunnel during DC etching. Besides, it can be seen that the distribution of the etched tunnel obtained in this work is more uniform than that of the etched tunnels generated in the literatures [23, 24], where the Zn nuclei or Zn layer were used for improving the distribution of the etched tunnels.

In order to investigate the effect of the merged tunnels on the specific surface area of etched aluminum foil, a model was built based on the typical merged tunnels in Fig.3. The basic structure unit of the etched tunnels formed at the initial stage was a cubic pit because of the high cubicity texture of aluminum foil substrate [25, 26]. So we used the cubic pit with the average size a as the elementary unit. The average sizes of the cubic pits in Fig.3 were evaluate by the Image Pro-plus software. And they were nearly the same value, namely 0.485±0.051 μm in Fig.3a, 0.483±0.032 μm in Fig.3b and 0.481±0.021μm in Fig.3c. The surface area of cubic pit is $5a^2$. Based on the segmentation of the typical merged tunnels, it approximatively consisted of nine cubic pits, as shown in Fig.4a. Based on the model, the effective surface area of the selected merged tunnels was filled with gray, as shown in Fig.4b. According to the calculation, the surface area of nine cubic pits and the selected merged tunnels were $45a^2$ and approximate $26a^2$, respectively. It can be seen that the merged tunnels can intensely reduce (about 42%) the surface area, resulting in the decrease of the specific surface area for the etched aluminum foil.

The density of the cubic pits in Fig.3, including the cubic pits used for constituting the merged tunnels, were evaluate by the Image Pro-plus software. They were 1.01×10^6 cm^{-2} in Fig.3a, 2.41×10^6 cm^{-2} in Fig.3b and 2.51×10^6 cm^{-2} (including 0.53×10^6 cm^{-2} used for constituting the merged tunnels) in Fig. 3c. It can be seen that the proportion of the cubic pits used for constituting the merged tunnels is too high to increase the specific surface area of the conventional aluminum foil. Compared with the conventional aluminum foil, the specific surface area for the aluminum foil with proper Sn nuclei was increased about 40.5%. So although the density of the cubic pits for the conventional aluminum foil was slightly higher than that for the aluminum foil with proper Sn nuclei, the specific surface area of the conventional aluminum foil was small compared to that of the aluminum foil with proper Sn nuclei.

The density of the Sn nuclei in Fig.2b was evaluate by the Image Pro-plus software. It was 2.38×10^6 cm^{-2} in Fig.2b. And the density of the Sn nuclei was approximately equal to that of etched tunnels in Fig.3b. The slightly excess etched tunnels were mainly generated by the flaws of the aluminum substrate. It means that the transfer of the uniformly distributed pattern of Sn nuclei to the aluminum substrate could be achieved by the anodically activating of aluminum foil. These results imply that the suitable Sn nuclei generated on aluminum surface can serve as the pitting initiation sites of aluminum foil, so that the distribution of the etched tunnels is improved clearly and subsequent the specific surface area of the etched aluminum foil can be increased remarkably.

3.3. Electrochemical characterization

Fig.5 shows the potentiodynamic polarization curves of the aluminum foils without or with Sn nuclei. It can be seen from Fig. 5 that the curves of anodic polarization gradually shifted to more positive potential, whereas that of the cathodic polarization gradually travelled to more negative region, which indicated that the anodic activation of the aluminum foil with uneven Sn nuclei was the weakest [27].

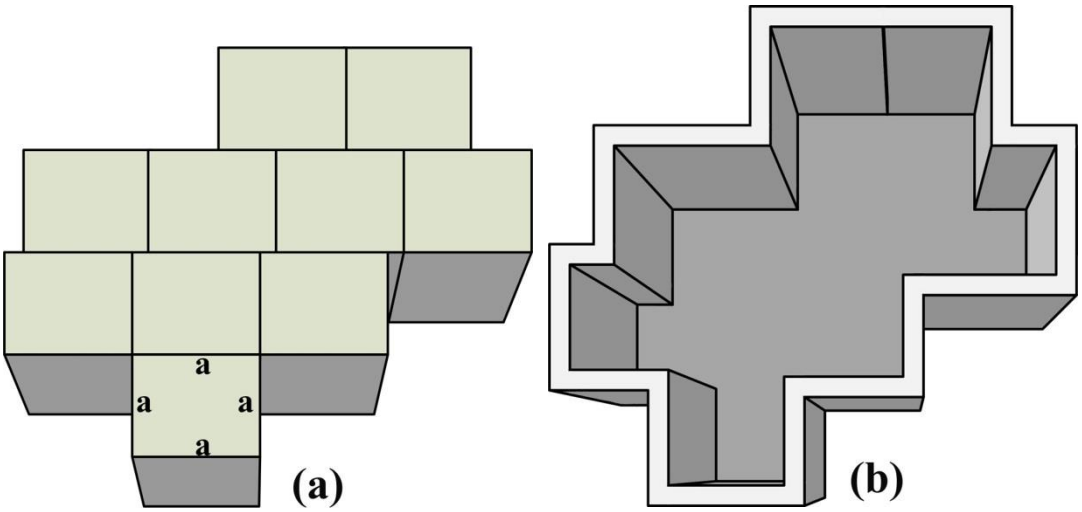

Figure 4. The model of the typical merged tunnels in Figure 3c: (a) the merged tunnels consisted with nine cubic pits and (b) the effective value of the surface area of the selected merged tunnels filled with gray. The size of cubic pits is a.

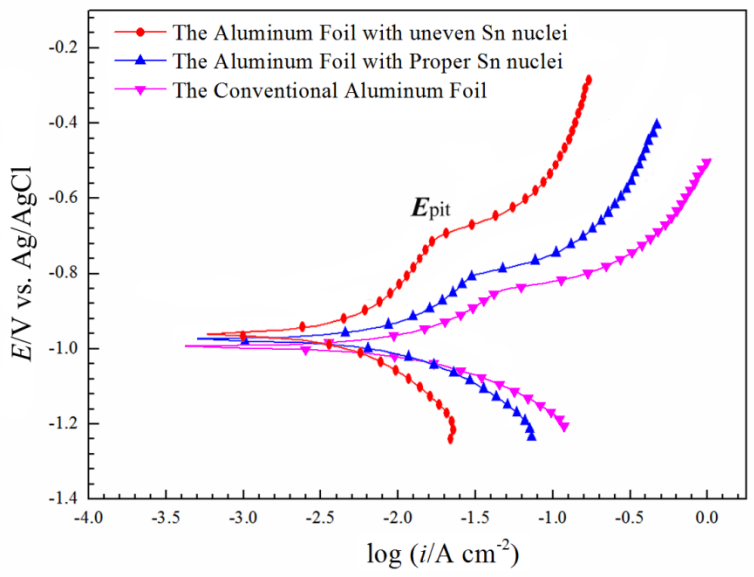

Figure 5. The Polarization curves of (a) the aluminum foil with uneven Sn nuclei, (b) the aluminum foil with proper Sn nuclei and (c) the conventional aluminum foil, respectively. The scanning rate was 10 mV s^{-1}.

The values of E_{pit} and the correspond pitting current for the aluminum foil with uneven Sn nuclei was larger than that of the convention aluminum foil. But the critical pitting potential of the aluminum foil with proper Sn nuclei, marked with E_{pit}, was slightly higher than that of the conventional aluminum foil. And the correspond pitting current was slightly lower than that of the conventional aluminum foil. It is indicated that the pitting initiation sites on the aluminum foil with Sn nuclei were lower than that of the conventional aluminum foil. This was verified also by the fact that the density of the etched tunnels on the aluminum foil with proper Sn nuclei was slightly lower than that of the conventional aluminum foil. And the density of the etched tunnels on the aluminum foil with uneven Sn nuclei was least.

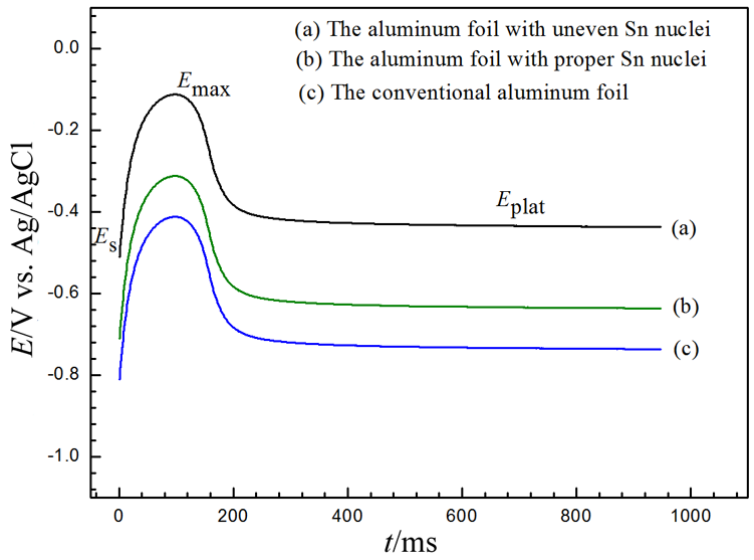

Figure 6. The initial potential transient of (a) the aluminum foil with uneven Sn nuclei, (b) the aluminum foil with proper Sn nuclei and (c) the conventional aluminum foil, respectively.

The initial potential transient of the aluminum foils without or with Sn nuclei is shown in Fig.6. The potential, induced by the ohmic drop and the electric double layer, rapidly increased from the initial potential. Then, due to the appearance of the film, the potential slightly rasied to the maximum value (E_{max}). The breakdown potential of the native oxide film, namely the electrochemical activation of the aluminum surface, can be estimated by the value of E_{max} [17, 28]. It can be seen that the value of E_{max} for the aluminum foil with proper Sn nuclei was slightly enhanced in contrast with that for the conventional aluminum foil, while that for the aluminum foil with uneven Sn nuclei was clearly increased to a greater extent. This is because the uneven Sn nuclei on aluminum surface caused limited surface activity, the value of E_{max} for the aluminum foil with uneven Sn nuclei was increased obviously. The surface activity of aluminum foil caused by the proper Sn nuclei was appropriate to induce tunnel pitting, resulting in the improvement of merged tunnels.

4. CONCLUSION

The electroless Sn nuclei were fabricated on aluminum surface and used for improving the distribution of the etched tunnels during DC etching. The work investigated here was based on the

relatively suitable density and uniform distribution of the localized Al-Sn micro-batteries on aluminum foil surface. That is, the appropriate density and distribution of the Sn nuclei fabricated on aluminum surface can serve as the initiation sites of etched tunnels, resulting in the distribution of the etched tunnels improved significantly. Although the density of the cubic pits on the conventional aluminum foil was slightly higher than that of aluminum foil with Sn nuclei, which was verified by the model evaluation and the potentiodynamic polarization, the specific surface area of the conventional aluminum foil was decreased remarkably. The reason is mainly due to the serious formation of the merged tunnels and the uneven distribution of etched tunnels. In comparison, the specific surface area of the aluminum foil with suitable Sn nuclei was enhanced eventually, based on the significant improvement of the merged tunnels and the distribution of the etched tunnels.

ACKNOWLEDGEMENTS
This research was supported by the Young People Fund of the Guangxi Science and Technology Department (No. 2018GXNSFBA050007 and No. 2018GXNSFBA050056), the Doctor's Scientific Research Foundation of Guilin University of Technology (No. GUTQDJJ2018050), and Science & Technology Base and Special Talent (GUIKE-AD19110066).

References

1. K.R. Herbert, and R. Alkire, *J. Electrochem. Soc.*, 135 (1988) 2146.
2. K. Hebert, *J. Electrochem. Soc.*, 135 (1988) 2447.
3. J. Kang, Y. Shin, and Y. Tak, *Electrochim. Acta*, 51 (2005) 1012.
4. M.A. Amin, S.S. Abd El Rehim, and E.F. El Sherbini, *Electrochim. Acta*, 51 (2006) 4754.
5. T. Fukushima, K. Nishio, and H. Masuda, *J. Electrochem. Soc.*, 157 (2010) 137.
6. H. Asoh, K. Nakamura, and S. Ono, *Electrochim. Acta*, 53 (2007) 83.
7. C.K. Chung, W.T. Chang, M.W. Liao, H.C. Chang, and C.T. Lee, *Electrochim. Acta*, 56 (2011) 6489.
8. S. Pan, L. Liang, B. Lu, and H. Li, *J. Alloys Compd.*, 823 (2020) 3795.
9. H.C. Chen, and B.L. Ou, *J. Mater. Sci.-Mater. Electron.*, 15 (2004) 819.
10. J.T.B. Gundersen, A. Aytaç, S. Ono, J.H. Nordlien, and K. Nişancıoğlu, *Corros. Sci.*, 46 (2004) 265.
11. Y.W. Keuong, J.H. Nordlien, S. Ono, and K. Nisancioglu, *J. Electrochem. Soc.*, 150 (2003) 547.
12. R.M. E. Sherif, K.M. Ismail, and W.A. Badawy, *Electrochim. Acta*, 49 (2004) 5139.
13. K. Arai, T. Suzuki, and T. Atsumi, *J. Electrochem. Soc.*, 132 (1985) 1667.
14. W. Lin, G.C. Tu, C.F. Lin, and Y.M. Peng, *Corros. Sci.*, 39 (1997) 1531.
15. W. Lin, G.C. Tu, and Y.M. Peng, *Corros. Sci.*, 38 (1996) 889.
16. K. Nishio, T. Fukushima, and H. Masuda, *Electrochem. Solid-State Lett.*, 9 (2006) 39.
17. T. Fukushima, K. Nishio, and H. Masuda, *Electrochem. Solid-State Lett.*, 13 (2010) 9.
18. H. Masuda, M. Tajima, and K. Nishio, *Chem. Lett.*, 31 (2002) 1150.
19. K.Q. Zhang, and S.S. Park, *Appl. Surf. Sci.*, 477 (2019) 47.
20. Y. Li, N. Peng, W. Shang, Y. Wen, and Y. He, *J. Electrochem. Soc.*, 167 (2020) 1508.
21. N. Peng, Y. Wen, and Y. He, *SN Appl. Sci.*, 1 (2019) 7.
22. J. Liu, J. Chen, X. Liu, Y. Yin, and C. Ban, *Anti-Corros. Methods Mater.*, 66 (2019) 7.
23. N. Peng, Y. He, H. Song, X. Yang, and X. Cai, *Corros. Sci.*, 91 (2015) 213.
24. C. Ban, Y. He, X. Shao, J. Du, and L. Wang, *Trans. Nonferrous Met. Soc. China*, 23 (2013) 3650.

25. J. Lee, J. Kim, H. Chung, and Y. Tak, *Corros. Sci.*, 51 (2009) 1501.
26. S.Q. Zhu, C.L. Ban, X.Q. Tao, W.Y. Chen, and L.J. Jiang, *J. Mater. Sci.-Mater. Electron.*, 26 (2015) 7.
27. B. Hu, Y. Sun, B. Guan, J. Zhao, H. Zhang, D. Zhu, K. Ma, and C. Cheng, *Appl. Surf. Sci.*, 392 (2017) 375.
28. N. Peng, Y. Wen, and Y. He, *Prog. Org. Coat.*, 127 (2019) 6.